POLARIMETRIC PARAMETER ACCURACY REQUIREMENTS OF SPACEBORNE SAR FOR THE OBSERVATION OF MID-LATITUDE IONOSPHERE ACTIVITIES

Jun Su Kim[1], Hiroatsu Sato[2], and Kostas Papathanassiou[1]
1) Microwaves and Radar Institute, DLR
2) Institute of Solar-Terrestrial Physics, DLR

DLR

SAR for Ionospheric Monitoring

- **High-latitude**
  - Strong scintillation effect over auroral oval due to precipitation of charged particles
  - High sensitivity of FR to TEC
  - Perpendicular alignment of the geomagnetic field to the orbit direction

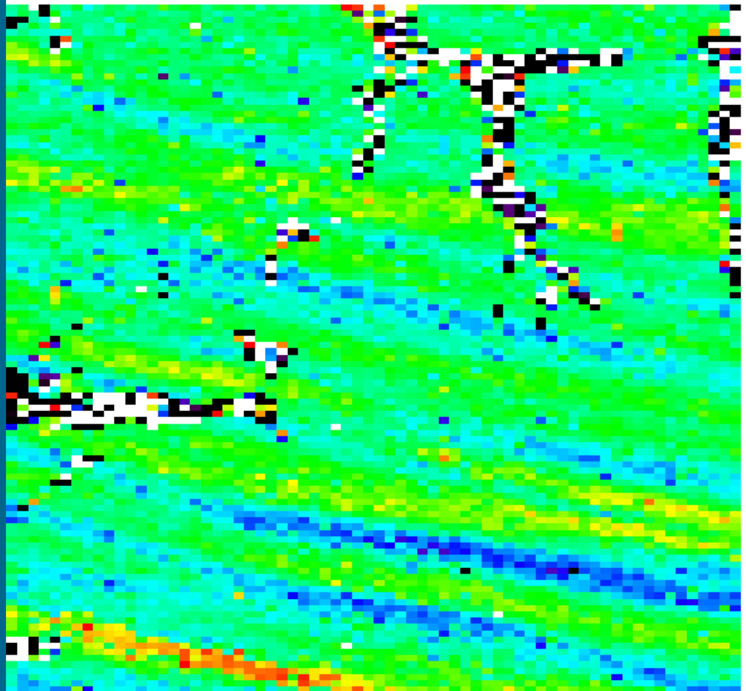

◄ Azimuth sub-band shift estimated over Tromsø −30 m to 30 m

- **Low-latitude**
  - Strong scintillation over post-sunset sector along plasma bubble
  - Insensitivity of Faraday rotation to TEC ~ low FR level
  - Strong Squint-FR relation
  - Parallel alignment of the geomagnetic field to the orbit direction

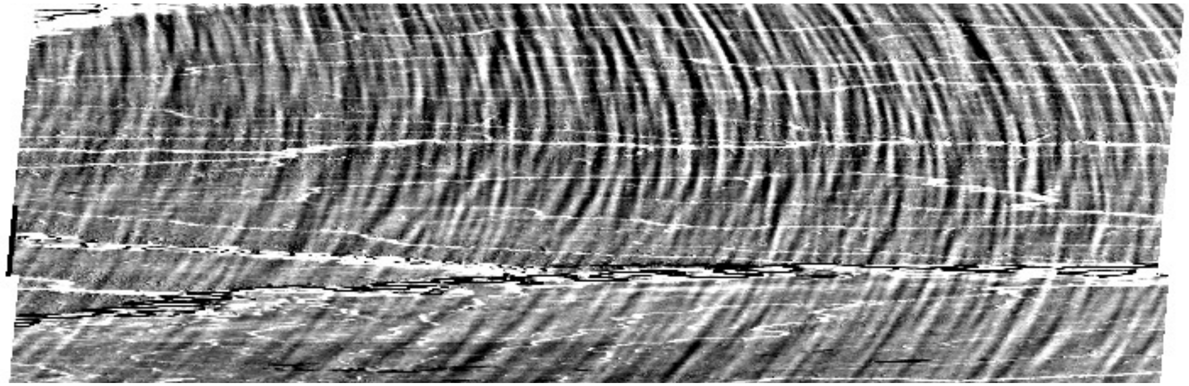

▲ Backscatter power modulation due to plasma bubbles over Amazon forest (−8 dB to −6 dB)

Mid-Latitude Ionospheric Disturbance

- **Travelling Ionospheric Disturbance (TID)**
- Waves of ionospheric undulation with < 1 TECU amplitude or less, and hundreds kilometer wavelengths.
- Observed from the systems of GPS networks.

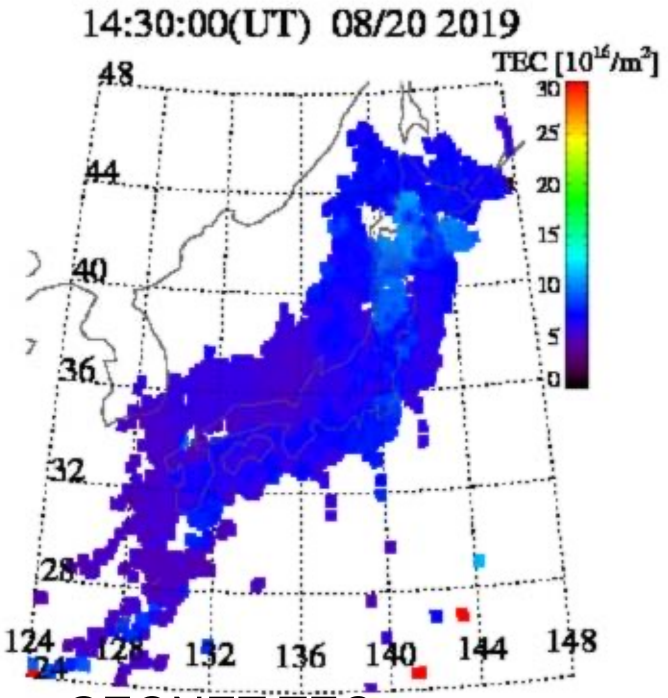

- GEONET TEC map

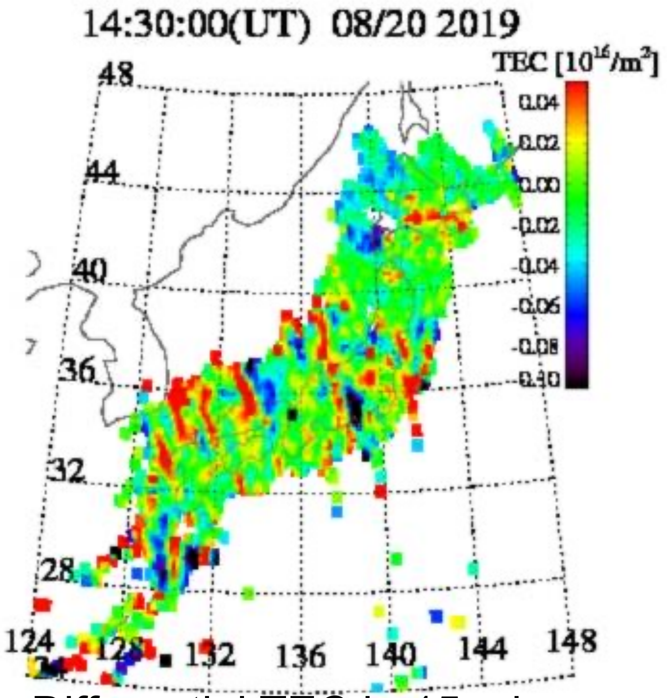

- Differential TEC in 15 min.

(Courtesy: Hiroatsu Sato @ DLR SO)

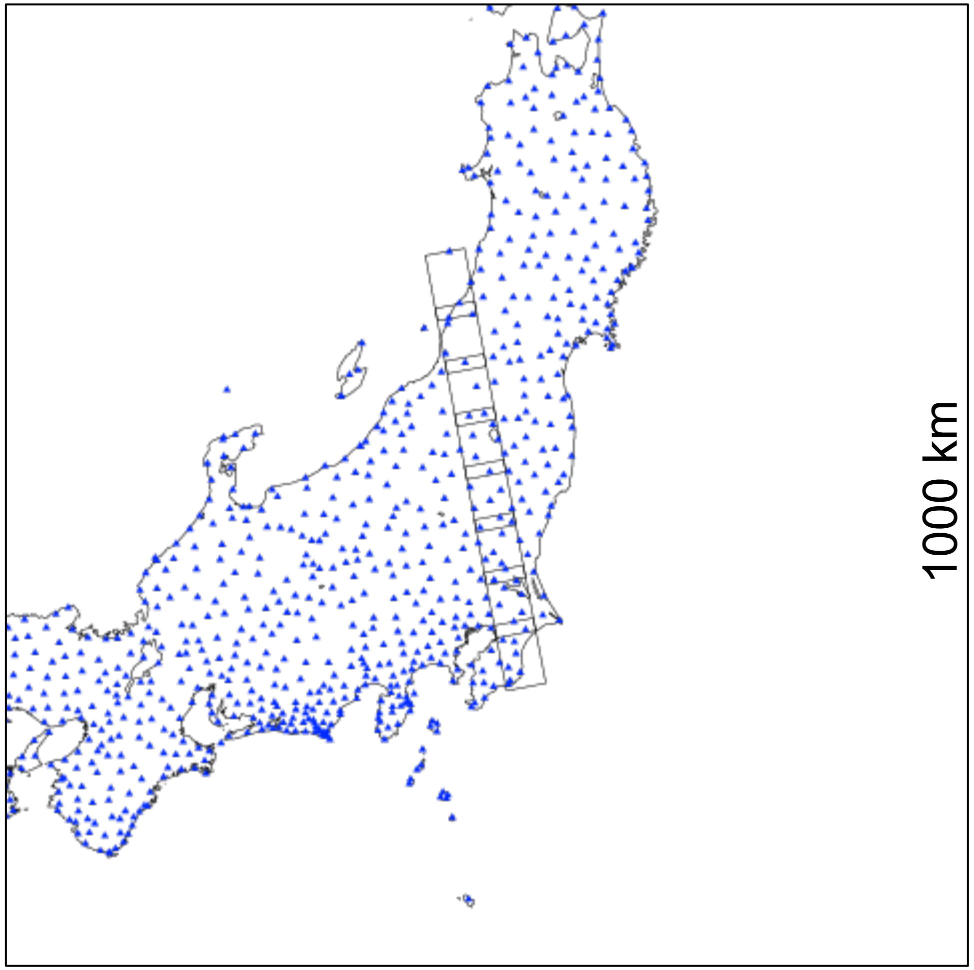

Footprints of ALOS-2/PALSAR-2 acquisition and GPS receiving stations (GEONET) over East Japan

SAR Data

Azimuth direction →

Acquisition on 2019.08.20 ($\vec{k}_p(t_0)$)

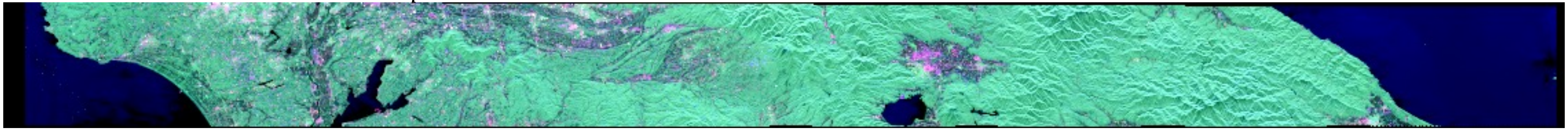

Acquisition on 2020.08.18 ($\vec{k}_p(t_1)$, where $t_1 = t_0 + 364$ days)

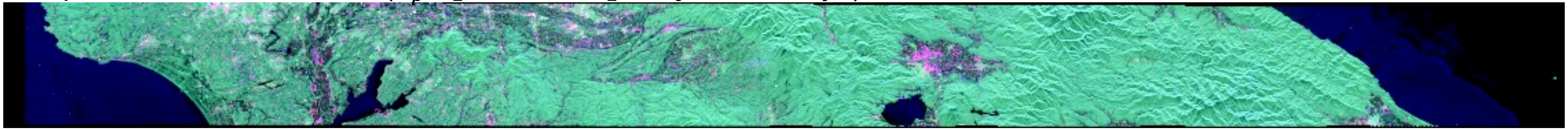

Difference ($\vec{k}_p(t_1) - \vec{k}_p(t_0)$)

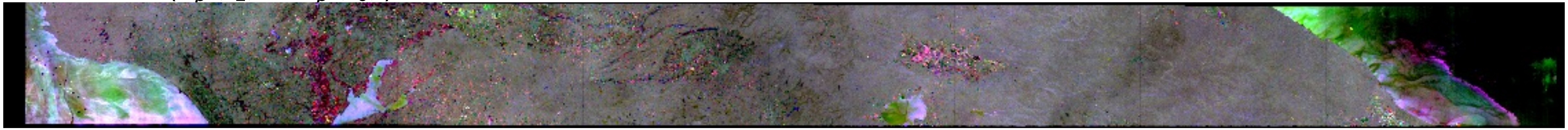

Estimation of FR

- **Rotation** of the polarization plane on linear basis.
- **Phase difference** of two circular waves on circular basis.
- FR is measured in terms of phase on circular basis: Bickel & Bates estimator.
- Estimated from quad-pol data as

$$4\Omega = \arg\langle S_{lr} \cdot S_{rl}^{*} \rangle$$

where

$$\begin{pmatrix} S_{rr} & S_{lr} \\ S_{rl} & S_{ll} \end{pmatrix} = \frac{1}{2} \begin{pmatrix} 1 & i \\ i & 1 \end{pmatrix} \begin{pmatrix} S_{hh} & S_{vh} \\ S_{hv} & S_{vv} \end{pmatrix} \begin{pmatrix} 1 & i \\ i & 1 \end{pmatrix}$$

- FR is directly proportional to
  TEC (integrated number density of free electrons) and,
  $\vec{B} \cdot \hat{\kappa}$ (parallel component of geomagnetic field to LOS).

$$\Omega = \zeta \frac{e\vec{B} \cdot \hat{\kappa}}{cmf^{2}} TEC$$

FR Estimates

Acquisition on 2019.08.20 (t_0)

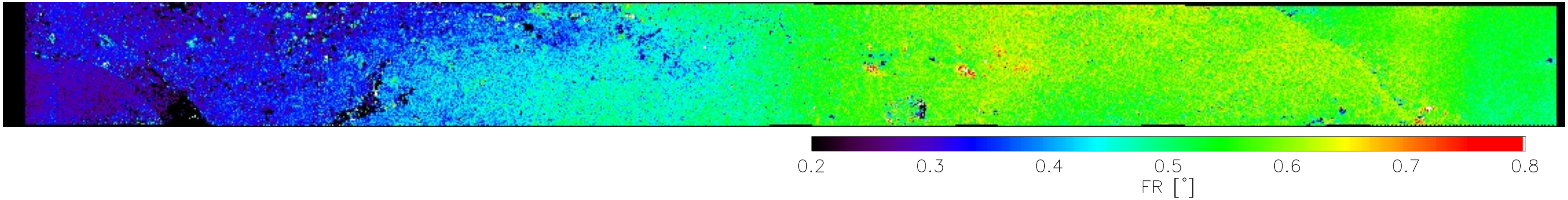

Acquisition on 2020.08.18 ($t_1 = t_0 + 364$ days)

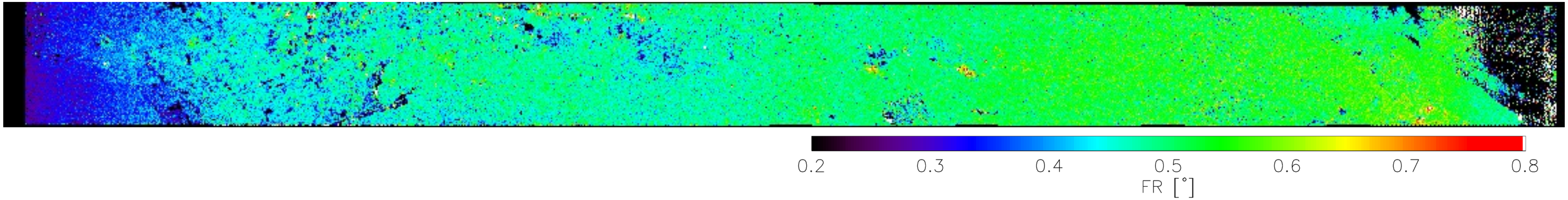

Difference ($\Omega(t_1) - \Omega(t_0)$)

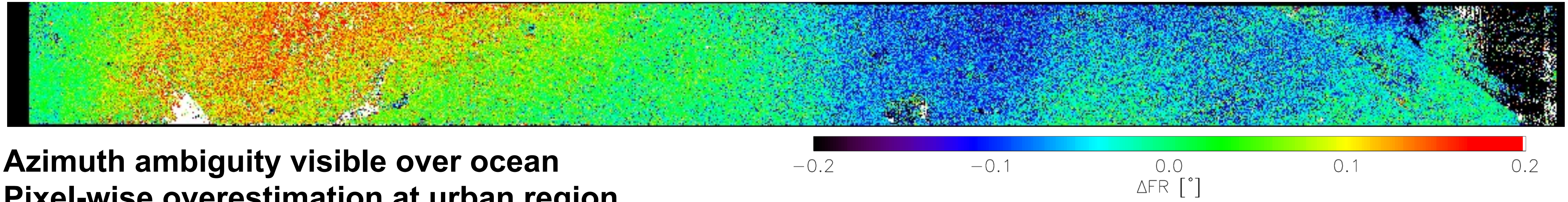

Azimuth ambiguity visible over ocean
Pixel-wise overestimation at urban region
Overestimation in 5th frame

Conversion from FR to TEC

Acquisition on 2019.08.20 (t_0)

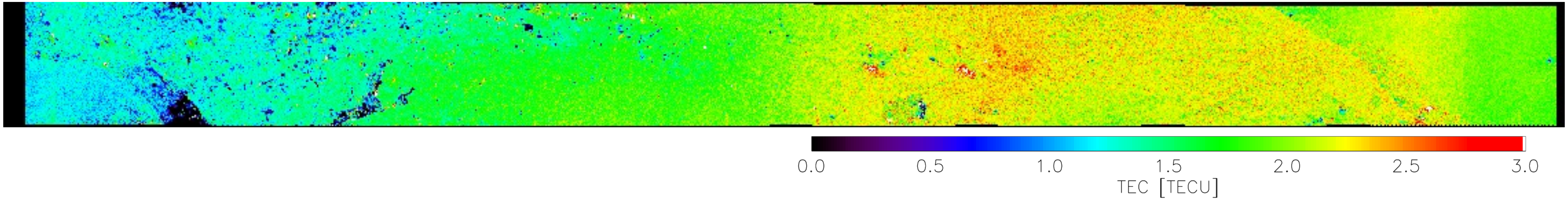

Acquisition on 2020.08.18 ($t_1 = t_0 + 364$ days)

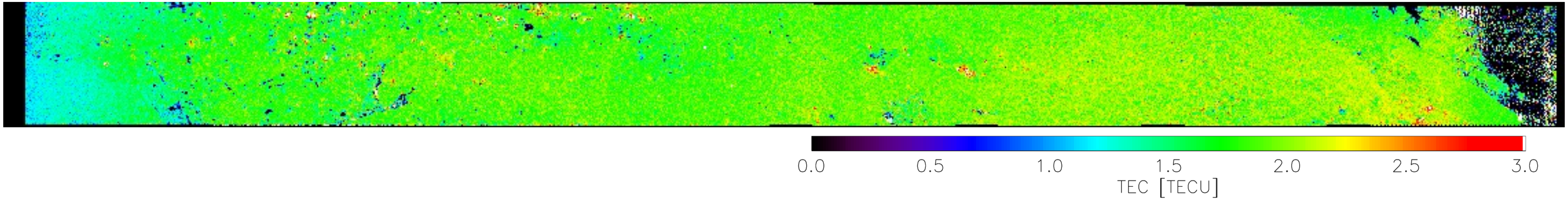

Parallel geomagnetic field ($\vec{B} \cdot \hat{\kappa}$)

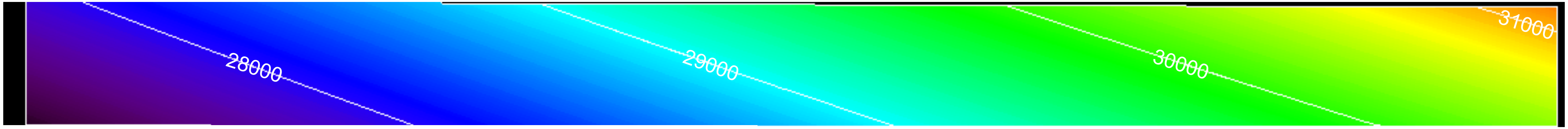

Conversion to TEC performed using $\vec{B} \cdot \hat{\kappa}$

10 % of FR increase is explained by $\vec{B} \cdot \hat{\kappa}$ change

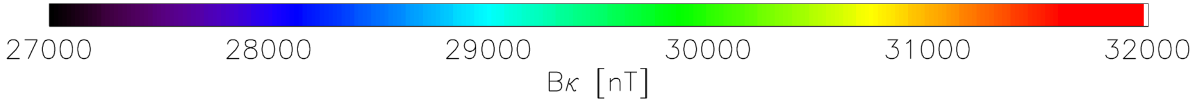

Interferograms

Interferogram ($\Delta t = 364$ days)

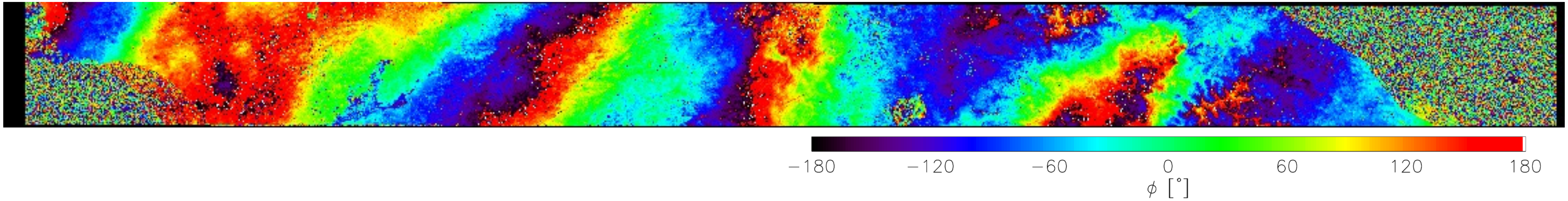

Coherence ($\Delta t = 364$ days)

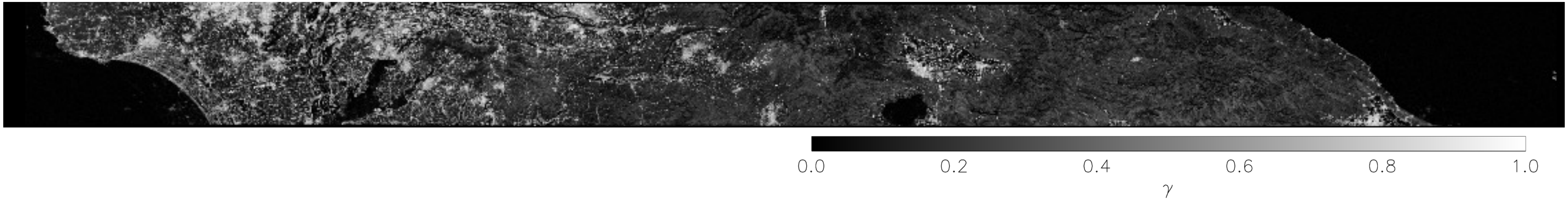

Pauli image

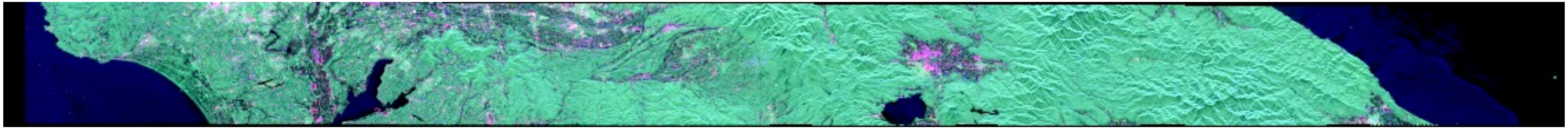

Alignment of fringes to the projection of geomagnetic field
Around three cycles of interferometric phase
Low coherence due to long temporal baseline

Differential TEC: Split Spectrum Method

- Dispersive nature of the ionosphere

$$\phi = \frac{4\pi\zeta}{cf}\Delta TEC$$

- The separation of ionospheric and non-dispersive contribution

$$\Delta\phi_{iono} = -\frac{f_0}{4\Delta f}\Delta\phi + \frac{1}{4}\Sigma\phi$$

$$\Delta\phi_{ndis} = \frac{f_0}{4\Delta f}\Delta\phi + \frac{1}{4}\Sigma\phi$$

where $\Delta\phi = \Delta\phi_H - \Delta\phi_L$, and $\Sigma\phi = \Delta\phi_H + \Delta\phi_L$.

- @ ALOS-2 PALSAR-2, $f_0 = 1.236$ GHz, $\Delta f = 13$ MHz.

Split Spectrum Method

Higher frequency interferogram ($f_{up} = 1.249$ GHz)

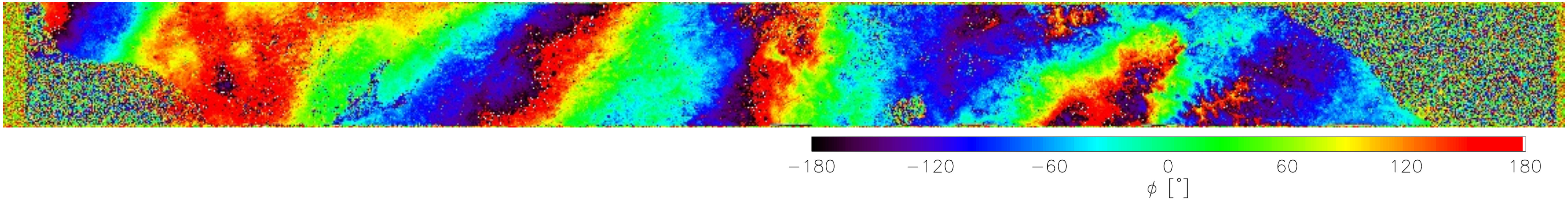

Lower frequency interferogram ($f_{dn} = 1.223$ GHz)

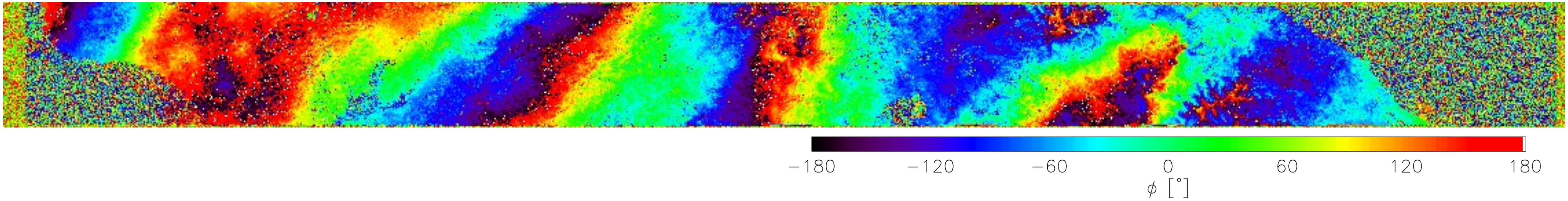

Ionospheric phase from TEC difference ($\mathrm{TEC}(t_1) - \mathrm{TEC}(t_0)$)

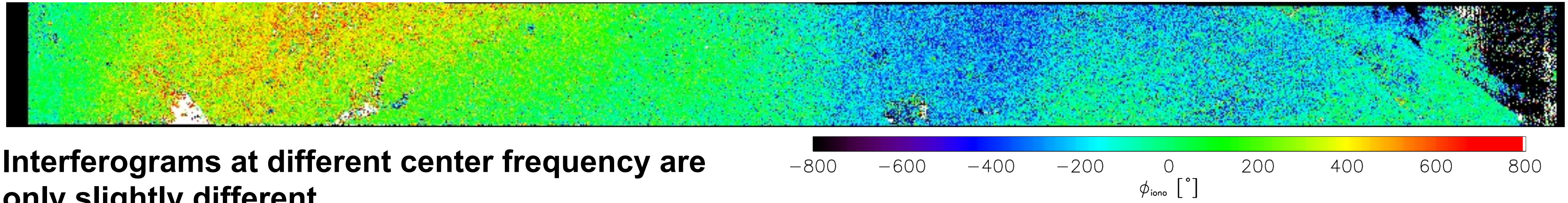

Interferograms at different center frequency are only slightly different.
Extracted ionospheric phase is similar to that from the FR difference.

Mid-latitude Ionospheric Disturbance is …

- Detectable using both polarimetry and interferometry.
- The differential TEC estimates from two methods are consistent.

- Identified problems:
  - A discontinuity at 5th frame in both polarimetry and interferometry.
  - There are strong azimuth ambiguity visible over ocean.
  - Consistent spiky FR biases over urban area.

NESZ Estimates

Acquisition on 2019.08.20 (t_0)

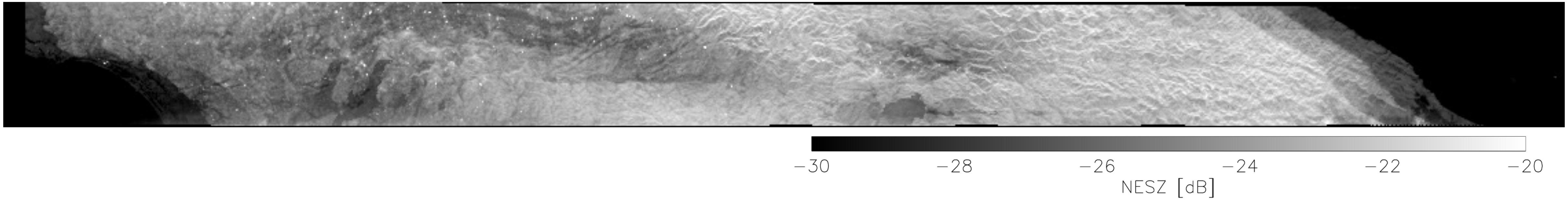

Acquisition on 2020.08.18 ($t_1 = t_0 + 364$ days)

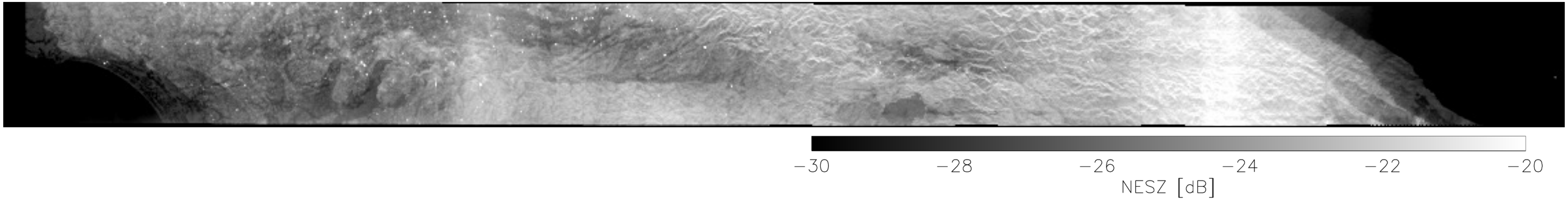

Ionospheric phase from TEC difference ($\mathrm{TEC}(t_1) - \mathrm{TEC}(t_0)$)

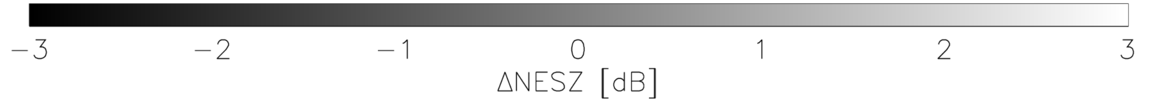

Estimated from the 4th eigenvalue of cov. matrix.
Strong azimuth ambiguity over ocean.
Their difference changes with azimuth time.

No special issue associated with 5th frame

Spiky Bias of FR Estimation

Acquisition on 2019.08.20 (t_0)

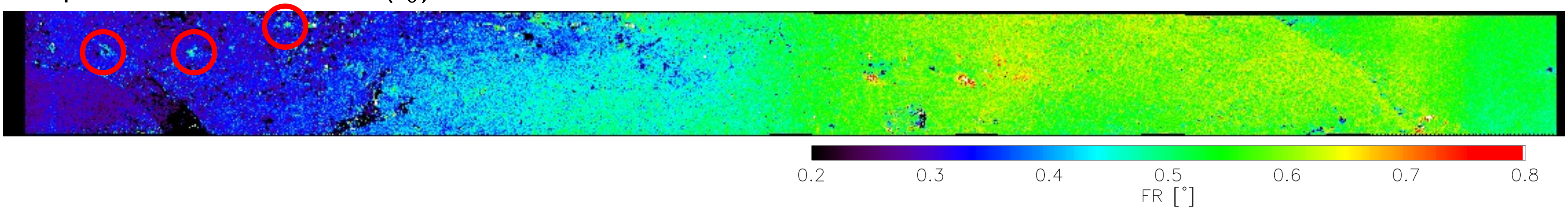

Acquisition on 2020.08.18 ($t_1 = t_0 + 364$ days)

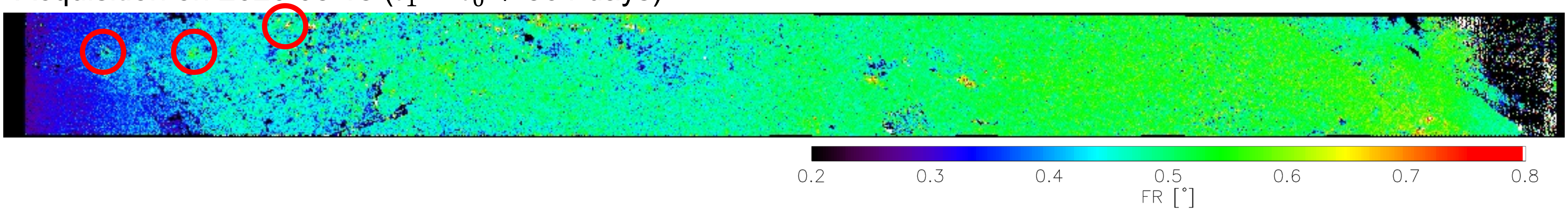

- Bias of FR estimate are **consistent**.
- Azimuth ambiguity of strong target interferers.
- Source of estimation bias are analysed in detail.

Practice of B&B Estimator

- FR in Bickel & Bates estimator

$$4\Omega = \arg\langle S_{lr} \cdot S_{rl}^{*} \rangle ,$$

where

$$\begin{pmatrix} S_{rr} & S_{lr} \\ S_{rl} & S_{ll} \end{pmatrix} = \frac{1}{2}\begin{pmatrix} 1 & i \\ i & 1 \end{pmatrix}\begin{pmatrix} S_{hh} & S_{vh} \\ S_{hv} & S_{vv} \end{pmatrix}\begin{pmatrix} 1 & i \\ i & 1 \end{pmatrix}$$

- Distribution of $S_{lr} \cdot S_{rl}^{*}$ in an estimation window: × is the mean of distribution

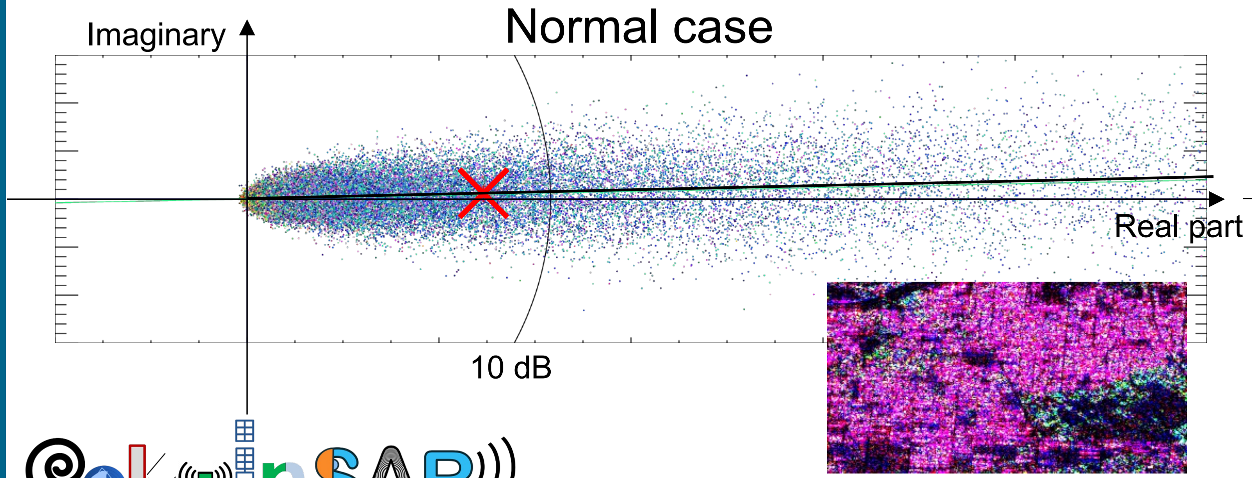

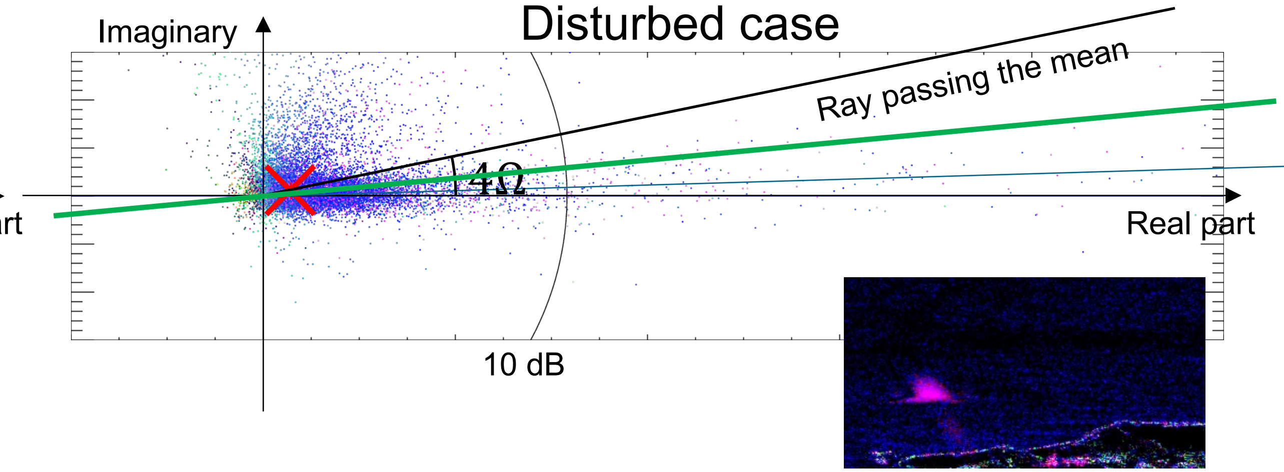

New FR Estimator

- Try to fit the distribution of $S_{lr} \cdot S_{rl}^*$ to a ray passing the origin with slope $\tan\theta$

$$x \sin\theta - y\cos\theta = 0$$

- Minimum square error method finds out such a relation

$$\sin 2\theta \sum_k \left(x_k^2 - y_k^2\right) - \cos 2\theta \sum_k 2x_k y_k = 0$$

Then,

$$8\Omega = \arg\left(\sum_k \left(x_k^2 - y_k^2\right) + i \sum_k 2x_k y_k\right)$$

where x_k and $y_k \in \mathbb{R}$ are real and imaginary parts of $S_{lr} \cdot S_{rl}^*$, respectively.

- Subscript k indicates k-th pixel in the estimation window.

New FR Estimator

Acquisition on 2019.08.20 (t_0)

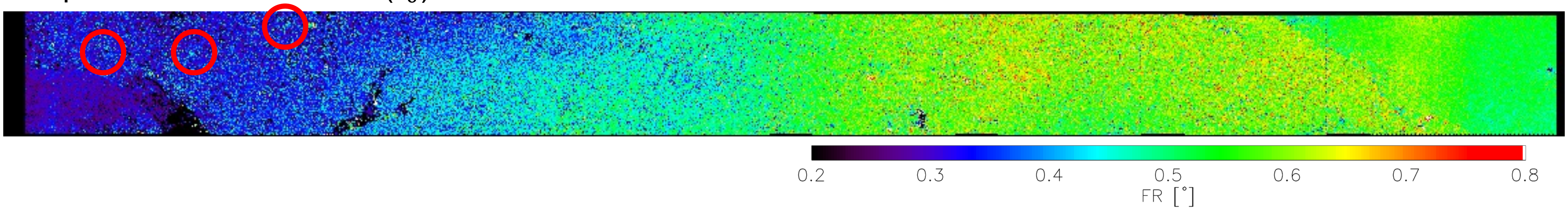

Acquisition on 2020.08.18 ($t_1 = t_0 + 364$ days)

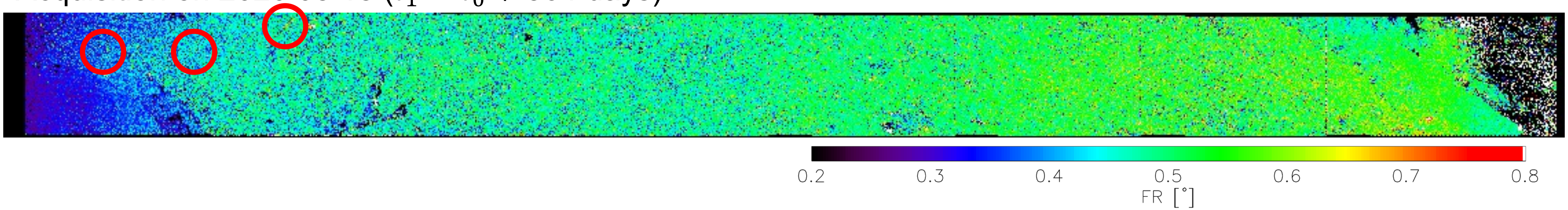

- Spiky biases are largely suppressed.
- But noisier than original estimator.
- Potentially applicable to urban conditions.
- Doubled wrapping cycle. Less optimal to lower frequency systems.

Estimation of Azimuth Sub-band Shift

Acquisition on 2019.08.20 (t_0)

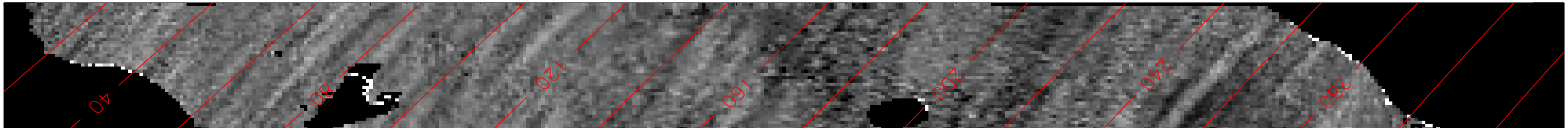

▲ **Azimuth direction subband shift (−1 m to 1 m)**

- At L-band 10 mTECU/ km ionospheric gradient induces 0.25 m azimuth shift.
- Azimuth sub-band shift estimate indicates quite non-quiet ionosphere.
- They are well aligned with projected geomagnetic field line (red lines).
- Geomagnetism seems govern the small scale ionospheric dynamics.
- Their effects are not visible either on polarimetric nor on interferometric ionosphere estimates.
- SAR is the only tool that can map the ionosphere with km-level resolution.

Conclusion and Remarks

- Mid-latitude ionospheric activity is observed by @ L-band.
- Polarimetric method and interferometric method yield **consistent** results.
  - Differential TEC levels are estimated from the FR difference, and from the dispersion on the interferogram.
  - A wave of ionospheric disturbance with amplitude of 0.5 TECU and wavelength 200 km was observed.
- **A new FR estimator** less sensitive to the az. ambiguity is proposed.
  - Hinted from the behavior of spiky bias of FR estimates due to azimuth ambiguity from strong urban scatterers.
  - New method presents higher level of noise, but suppresses spiky biases.
- Kilometer-scale ionospheric irregularities exist, and observed by using the azimuth sub-band shift estimation.
  - Conventional polarimetric or interferometric methods cannot detect them.
  - Conventional ionosphere monitoring tools also cannot observe them.

THANK YOU VERY MUCH FOR YOUR ATTENTION AND JAXA

Jun Su Kim[1), Hiroatsu Sato[2), and Kostas Papathanassiou[1)
1) Microwaves and Radar Institute, DLR
2) Institute of Solar-Terrestrial Physics, DLR

DLR